



International Conference on Sustainable and Intelligent Manufacturing, RESIM 2016, 14-17  
December 2016, Leiria, Portugal

## Development of heterogeneous structures with Polycaprolactone-Alginate using a new 3D printing system – BioMED<sub>beta</sub>: design and processing

Biscaia S.<sup>a</sup>, Dabrowska E.<sup>b</sup>, Tojeira A.<sup>a</sup>, Horta J.<sup>a</sup>, Carreira P.<sup>a</sup>, Morouço P.<sup>a</sup>, Mateus A.<sup>a</sup>,  
Alves N.<sup>a,\*</sup>

<sup>a</sup>Centre for Rapid and Sustainable Product Development, Polytechnic Institute of Leiria, Portugal

<sup>b</sup>Warsaw University of Technology

---

### Abstract

Direct Digital Manufacturing of implantable biomedical devices is the strategy for designing and constructing three dimensional (3D) structures. DDM (i.e., biomanufacturing) technologies have been widely used to construct complex 3D structures (scaffolds), where chemicals, biomaterials, and cells are deposited in a layer-by-layer fashion. These technologies control size, microarchitecture and pores interconnectivity in scaffolds, essential to transporting oxygen and nutrients for cell survival. As the Tissue engineering field progresses, new types of printers have been designed to accomplish functional engineered tissue constructs. However, the availability of innovative 3D biomanufacturing technologies for hard tissue and organ engineering is scarce and with several equipment limitations. In this work, a new biomanufacturing system, BioMED<sub>beta</sub>, composed of three different fabrication modules (thermoplastic micro-extrusion, multi-head deposition of hydrogels and electrospinning) was used to fabricate (3D) scaffolds using layer-by-layer alternated deposition of polycaprolactone and alginate hydrogel. The BioMED<sub>beta</sub> system demonstrates the possibility of obtaining scaffolds with well-defined architecture, using both natural and synthetic polymers. Nevertheless, there are still parameters to optimize related with the design of 3D constructs and materials processing.

© 2017 Published by Elsevier B.V. This is an open access article under the CC BY-NC-ND license (<http://creativecommons.org/licenses/by-nc-nd/4.0/>).

Peer-review under responsibility of the scientific committee of the International Conference on Sustainable and Intelligent Manufacturing

*Keywords:* Tissue engineering, Biomanufacturing, Bioprinting, Micro-extrusion, Heterogenous scaffolds

---

\* Corresponding author. Tel.: +351-244-569441; fax: +351-244-569444.  
E-mail address: [nuno.alves@ipleiria.pt](mailto:nuno.alves@ipleiria.pt)

## 1. Introduction

Tissue engineering (TE) aims to build functional tissue or organ substitutes, through tissue regeneration or total substitution using a patient's autologous cells. This strategy includes the use of support structures to guide tissue formation. Research has been focused on the development of scaffolds which provides biomechanical support for cell adhesion, proliferation and differentiation. Such constructs are biocompatible devices, with controlled biodegradability rate and high porosity and pore interconnectivity to promote proper tissue vascularization [1-5]. Recent studies have underlined the development of heterogeneous 3D structures as one of the most promising TE strategies. However, heterogeneous tridimensional scaffold development is significantly dependent on diversified biomanufacturing systems and technologies.

3D Bioprinting is a DDM technique designed to tri-dimensionally pattern deposition of cell-laden systems (e.g. hydrogels) using additive manufacturing (layer-by-layer) construction principles to obtain functional tissues such heart tissue, blood vessels, heart valve, trachea, etc.) [6]. Apart from the simplicity of the concept, bioprinting is extremely dependent on precise position cell-carrying systems, availability of printable biomaterials at low temperatures, cell sources and growth factors. Bioprinting can be subdivided in extrusion-based bioprinting (EBB), inkjet, and laser based –technologies: extrusion consists of solid-freeform fabrication based on continuous dispensing of cell aggregates, cell loaded biomaterials, micro-carrier, etc. EBB technologies are generally superior in deposition volume, cell density and printing speed. In opposition, commercially available extrusion-based bioprinters have very limited resolution (~100 $\mu$ m) compromising the cell patterning and organization [7]. Inkjet technology consists on drop-on-demand (non-contacting) system with varying droplet sizes determined by temperature, frequency of pressure pulses and ink rheological properties. Individual droplets are ejected in consequence of thermal (thermal bioprinting), piezoelectric (piezoelectric bioprinting) or electrostatics (electrostatic bioprinting) actuation which surpasses the ink surface tension [8]. Lastly, laser based-technologies (LaBP) involve cell transfer from a “cell solution” which sublimates under exposure to a pulsed laser releasing the underlying biological substances. This process provides a higher resolution and great cell viability [9].

A melt-extrusion-based technique, i.e., Fused Deposition Modelling (FDM), deposits thermoplastics filaments, with diameters ranging from 100 to 500 $\mu$ m, through an extrusion nozzle heated to a temperature higher than the polymer's melting temperature. The liquefied polymer is drawn onto a platform it solidifies culminating with scaffolds with increased mechanical properties suitable for hard tissue applications (i.e. bone) [10]. A significant drawback of melt-extrusion techniques relate to the inability of cell to survive or biomolecules to retain normal activity in consequence of high temperature of the systems; however it has been proved that FDM scaffold are beneficial in mechanically supporting the cells avoiding structure collapse while tissue is forming [11].

Smaller polymer fibers with typical diameters of 5-30 $\mu$ m are made using electrospinning processes: melt or solution-based. Melt electrospinning consists in ejecting liquefied polymer from a spinneret by application of a high potential difference applied between its orifice and the collector. The polymer melt fibres are then solidified at the base of the collector with random alignment. As alternative, solution-based electrospinning allow the use of polymers which do not withstand high temperatures, but a solvent instead [12].

Because native tissues present heterogeneous characteristics, heterogeneous scaffold fabrication implies the combination of multiple techniques to obtain different scales of microstructure and properties. Multi-head systems have been studied to obtain heterogeneous structures, particularly, by combining biodegradable thermoplastics and hydrogels materials [13-16]. However, such apparatus present limitations regarding their bulk dimensions, limited possibility of techniques and materials combination, reduced control over the geometric and structural tri-dimensional parameters, complex operating system, etc.

BioMED<sub>beta</sub> equipment allows combination of different biomaterials for construction of functionally graded scaffolds with well-defined architectures using a wider range of materials and three different biomanufacturing techniques: micro-extrusion system, a multi-head hydrogel dispensing system and electrospinning modules. This work aims to study and validate the BioMED<sub>beta</sub> equipment as a new biomanufacturing system for construction of heterogeneous tridimensional scaffolds. Due to the complexity of the validation process, this report will only focus on the development of heterogeneous scaffolds by combination of micro-extrusion (thermoplastic) and multi-head dispensing (hydrogels) techniques.

### Nomenclature

DV	Deposition velocity
PCL	Polycaprolactone
SA	Sodium alginate
SRV	Screw rotation velocity

## 2. BioMED<sub>beta</sub> system configuration

The BioMED<sub>beta</sub> is a new biomanufacturing system which integrates and synchronizes three biomanufacturing techniques to obtain heterogeneous tri-dimensional constructs: multi-head dispensing system, micro-extrusion system and electrospinning.

The multi-head dispensing system (Fig. 1a) was designed to dispense gel like biomaterials (e.g. alginates, chitosan, hyaluronic, etc.), actuated by time regulated air pressure into the syringe cartridge, driving the material to flow from the nozzle. Due to biomaterials and cells sensibility to temperature and shear, the multi-head dispensing system operates at room temperature and low pressure conditions.

The micro-extrusion system consists in a biocompatible polymer liquefying apparatus coupled to a screw and nozzle head to create polymer melt flow and subsequent deposition onto a platform. This technique is highly reproducible and enables to obtain constructs with higher mechanical properties, controlled porosity (pore size, shape and distribution) and lower degradation rates (Fig. 1b).

Finally, the electrospinning system was designed to obtain polymer meshes with nano- to micro-scale fiber dimension from polymer solutions (Fig. 1c). Fibers are formed by application of an electric potential between the nozzle and collector (system platform) creating a force higher than the surface tension of the polymer solution of a polymer droplet at the tip of the nozzle. Such phenomenon leads to the polymer jet formation which is further elongated by electrostatic interactions creating very long fibers with small diameter. Fibre solidification occurs by solvent evaporation during fibre elongation [17].

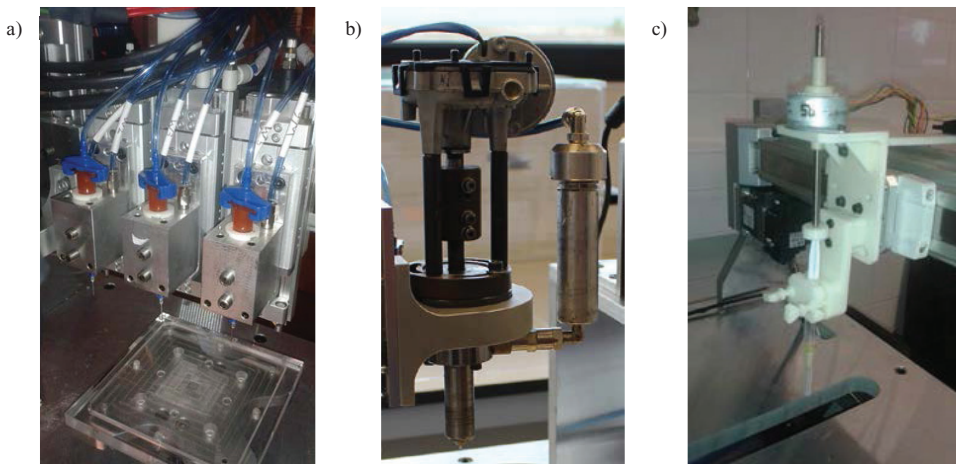


Fig. 1. BioMED<sub>beta</sub> system: a) multi-head dispensing, b) micro-extrusion module and c) electrospinning modules.

### 3. Materials and methods

#### 3.1. Materials

Polycaprolactone CAPA® 6500 (Mw: 50,000 Da) was purchased from Perstorp Caprolactones (Cheshire, UK). Sodium alginate solutions were prepared by dissolving 4.5%, 6% and 7%w/v sodium alginate (PROLABO BDH: 27660.296) in deionized water, and crosslinking solution was prepared by dissolving calcium chloride di-hydrate ( $\text{CaCl}_2 \cdot \text{H}_2\text{O}$ ) (Honeywell Fluka; Mw 147,01 g/mol) at a concentration of 0.6 M in deionized water to obtain an hydrogel.

#### 3.2. Preliminary data on thermoplastic and hydrogel deposition

The development of a new fiber-based biomanufacturing system requires validation studies of the dimensional accuracy of the thermoplastic (PCL) and hydrogel (SA) deposited samples. Fiber optical microscopy was performed using a Crocus 5MP MCX100 microscope (Micros, Austria) at a magnification of 4×. Different set of thermoplastic and hydrogel samples were made by varying deposition velocity (both PCL and SA), screw rotation velocity (only PCL) and pressure (SA). A similar study was conducted to study the influence of alginate crosslinking with  $\text{CaCl}_2$  solutions for a period of 5 minutes on fiber cross section. Intra-sample and inter-samples measurements of sample groups were made in tenfold and triplicates, respectively.

#### 3.3. Heterogeneous scaffold fabrication

PCL/SA hybrid constructs (dimension of 15x15 mm) consisted of alternating steps of synthetic polymer and hydrogel printing. The PCL polymer was melted by heating to 90°C and subsequently dispensed through a nozzle with a diameter of 400µm using air pressure of 6 bar, screw rotation velocity of 11 rpm and deposition velocity of 500 mm/min. Sodium alginate (4.5; 6 and 7% (w/v)) was dispensed in the spaces between the filaments of the PCL at room temperature, using a deposition speed of 500mm/min, air pressure between 2-5 bar and nozzle diameter of 400µm. The second layer was deposited at a 90 angle. After the production of scaffolds with 2 and 8 layers, the alginate was cross-linked with  $\text{CaCl}_2$  (0.6M).

#### 3.4. Statistical Analysis

Normality was checked by Shapiro-Wilk tests. Descriptive statistics (mean and standard deviation) were calculated for all dependent variables. The significance of differences between types of scaffolds was evaluated by analysis of variance (one-way ANOVA) and linear regression was determined for each printing parameter. The significance of differences resulting from crosslinking of the SA samples was evaluated by paired *t*-test. All statistical procedures were performed using SigmaPlot 12.0. The level of statistical significance was set at 95% ( $p < 0.05$ ).

## 4. Results and Discussion

#### 4.1. Preliminary data on PCL and SA deposition

Preliminary studies were conducted using the micro-extrusion system to construct PCL fibers at different deposition and screw rotation velocities. For example, as shown in Fig. 2a, we found that the cross section of the fibers varies significantly with the deposition velocity and that higher velocities lead to smaller cross section. At fixed feed rate (i.e., screw rotation velocity) there is some deformation of the polymer fibers during the deposition, decreasing the fiber cross section. The results regarding the deposition velocity of extruded PCL fibers were significant ( $p < 0.05$ ) according to the linear regression analysis ( $R^2 = 0.905$ ). Similar analysis (Fig. 2b) was performed to determine linearity in variation of the SRV parameter of the micro-extrusion process which did not

confirmed linear tendency between different groups of fibers ( $p > 0.05$ ;  $R^2 = 0.891$ ).

A similar study was performed with non-cross-linked SA samples. Fig. 3a illustrates the variation of SA fibers cross section with deposition velocity. Regression analysis demonstrated that fiber cross section of SA samples were linearly dependent on the deposition velocity ( $p < 0.05$ ;  $R^2 = 0.965$ ). Fig. 3b, similarly to the SRV in PCL samples, shows that higher pressures lead to increased hydrogel cross section ( $p < 0.05$ ).

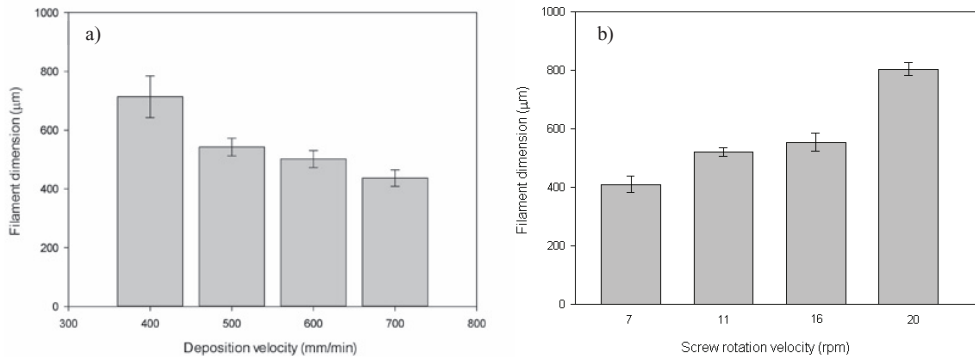


Fig. 2. PCL fiber dimension with variation of micro-extrusion parameters: a) deposition velocity and b) screw rotation velocity.

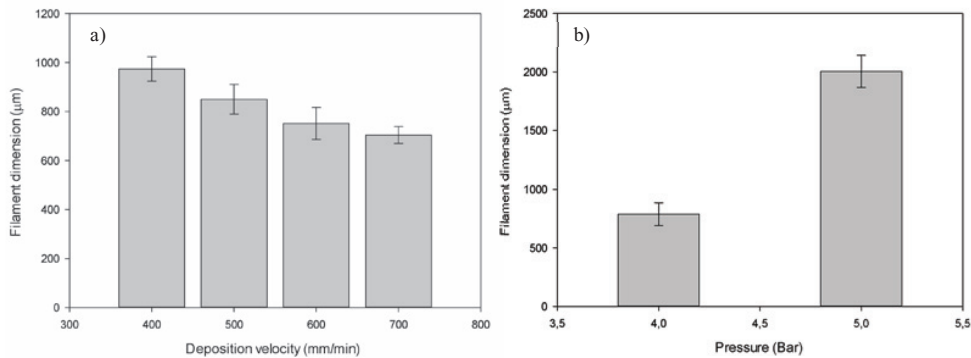


Fig. 3. SA fiber dimension with variation of multi-head dispensing system parameters: a) deposition velocity and b) pressure.

We also studied the influence of ionic crosslinking treatment on the SA fibers. As shown in Fig. 4, we verify that crosslinking treatment increased significantly SA fibers cross section ( $t = -3,655$ ; d.f. = 9;  $p = 0,005$ , paired  $t$ -test). These results are attributed to the high level of water uptake, of the cross-linked samples causing swelling of the alginate fibers which is a characteristic of hydrogels.

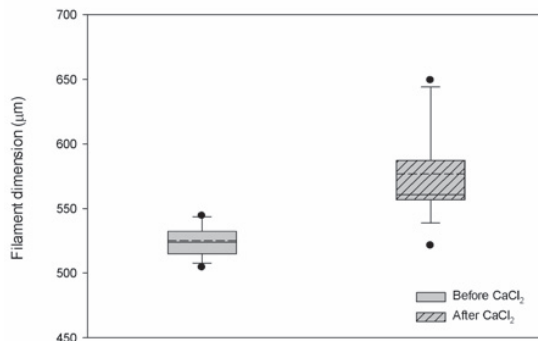


Fig. 4. Variation of hydrogel dimensions with ionic crosslinking treatment with CaCl<sub>2</sub> solution: (box plot details: full line: median, dashed line: mean, •: 5th and 95th percentiles).

#### 4.2. Multi-layer heterogeneous scaffolds

Fig. 5 demonstrates the materials (PCL and SA, respectively) being alternately deposited, using the fused deposition system and multi-head dispensing system. After printing, heterogeneous two and eight layer-scaffolds were submitted to alginate crosslinking with CaCl<sub>2</sub> solution.

Micrographs were taken to observe the internal structure of the constructs. Experiments (Fig. 6) demonstrate SA filaments exactly positioned between the PCL filaments indicating good coordination and alternation between the micro-extrusion and multi-head dispensing system during the construction of heterogeneous scaffolds.

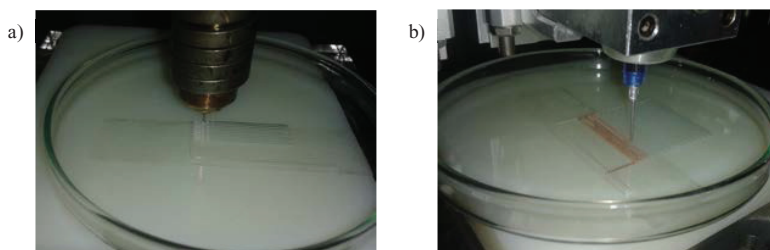


Fig. 5. Multi-nozzle heterogeneous material deposition: a) thermoplastic material and b) hydrogel.

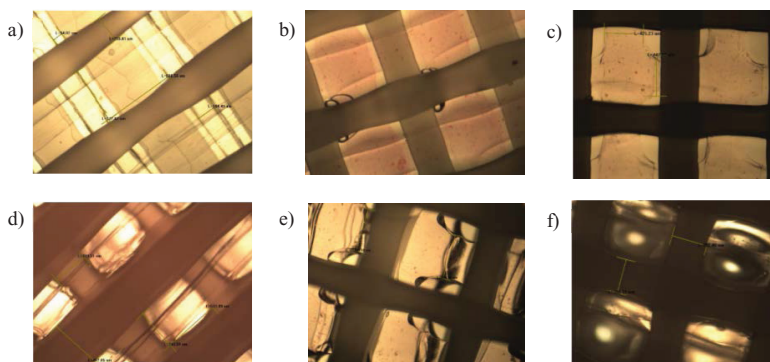


Fig. 6. Micrographs of PCL/SA scaffolds with 2 layers with SA hydrogel at concentration of: (a) 4,5%(w/v); (b) 6%(w/v); (c) 7%(w/v); scaffolds with 8 layers with SA hydrogel at concentration of: (d) 4,5%(w/v); (e) 6%(w/v); (f) 7%(w/v).

Results on two layer-scaffolds (Fig. 6 a, b and c) show good control over the geometric parameters of the fibers and pores. Eight layer-scaffolds present similar results in scaffolds with alginate at lower concentration (Fig. 6d). At higher SA concentrations and increment of number of layers, there is significant difficulty to maintain geometric accuracy of scaffolds due to the SA fibers slithering towards the lower layers and lack of control  $\text{Ca}^{2+}$  migration within the structure during crosslinking. Scaffolds obtained with PCL and SA 6% (w/v) present the most accurate filament size (around 400 $\mu\text{m}$ ) which corresponds to the nozzles diameter used during printing (Table 1).

Table 1. Filament dimensions of the heterogeneous scaffolds.

Scaffold composition	N.º of layers	PCL filament ( $\mu\text{m}$ )	SA filament ( $\mu\text{m}$ )
PCL/SA 4.5%	2	324,50 $\pm$ 20,51	192,11 $\pm$ 11,17
	8	320,12 $\pm$ 13,98	-
PCL/SA 6%	2	424,60 $\pm$ 5,01	397,00 $\pm$ 3,92
	8	372,07 $\pm$ 1,29	-
PCL/SA 7%	2	333,66 $\pm$ 3,32	433,62 $\pm$ 11,86
	8	392,16 $\pm$ 13,29	-

## 5. Conclusions

BioMED<sub>beta</sub> system demonstrates the possibility to obtain scaffolds with well-defined architecture, using both natural and synthetic polymers. Nevertheless, there are still parameters to optimize related with the design of 3D constructs with higher number of layers. Further validation tests must be performed, namely relating to temperature influence on both thermoplastic and hydrogel fiber deposition and test of versatility upon other materials processing.

## Acknowledgements

The research was funded by the projects *insitu.Biomas* (project reference: POCI-01-0247-FEDER-017771) from the Portuguese National Innovation Agency; and UID/Multi/04044/2013 from the Portuguese Foundation for Science and Technology.

## References

- [1] X. Wang, Q. Ao, X. Tian, J. Fan, Y. Wei, W. Hou, H. Tong, S. Bai, *Materials* 9 (2016) 1–23.
- [2] A. Atala, K. Richardson, *Biochemical Society* (2016), 24–27.
- [3] S. Biscaia, P. Carreira, J. Horta, P. Morouço, A. Mateus, N. Alves, *In International Conference on Direct Digital Manufacturing and Polymers, Abstracts proceedings ICDDMAP 2015* (2015), 62.
- [4] G. Gao, X. Cui, *Biotechnol. Lett.*, 38 (2016) 203–211.
- [5] X. Zhang, Y. Xhang, *Cell Biochem. Biophys.*, 72 (2015) 777–782.
- [6] X. Li, J. He, W. Zhang, N. Jiang, D. Li, *Materials* 9 (2016) 1–17.
- [7] I.T. Ozbolat, M. Hospodiuk, *Biomaterials* 76 (2016) 321–343.
- [8] H. Gudapati, M. Dey, I. Ozbolat, *Biomaterials* 102 (2016) 20–42.
- [9] M. Gruene, M Pflaum, *Tissue Eng Part C Methods* 17 (2011) 973–982.
- [10] C. Mota, D. Puppi, F. Chiellini, E. Chiellini, *J. Tissue Eng. Regen. Med.*, 9 (2015) 174–190.
- [11] G.-H. Wu, S.-H. Hsu, *J. Med. Biol. Eng.* 35 (2015) 285–292.
- [12] P.D. Dalton, M.L. Muerza-Cascante, D.W. Hutmacher, in: G.R. Mitchell (Ed.), *Electrospinning: Principles, Practice and Possibilities*, The Royal Society of Chemistry, United Kingdom, 2015, pp. 100–119.
- [13] J. Kundu, J.-H. Shim, J. Jang, S.-W. Kim, D.-W. Cho, *J. Tissue Eng. Regen. Med.* 9 (2013) 1286–1297.
- [14] J.W. Jung, J.S. Lee, *Sci. Rep.* 6: 21685 (2016) 1–9.
- [15] J.Y. Kim, D.-W. Cho, *Microelectron. Eng.* 86 (2009) 1447–1450.
- [16] T. Xu, K.W. Binder, M.Z. Albanna, D. Dice, W. Zhao, J.J. Yoo, A. Atala, *Biofabrication* 5 (2013) 1–10.
- [17] J. Lannuti, D. Reneker, T. Ma, D. Tomasko, D. Farson, *Mater. Sci. Eng. C* (2007), 504–509.